

EXACT ANALYSIS OF MHD CASSON FLUID FLOW PAST AN EXPONENTIALLY ACCELERATED VERTICAL PLATE IN A POROUS MEDIUM WITH RADIATION ABSORPTION, HEAT GENERATION, AND DIFFUSION-THERMO EFFECTS WITH THERMAL AND SOLUTAL RAMPED CONDITIONS

Dibya Jyoti Saikia^{a,b*}, Nazibuddin Ahmed^c, Ardhendu Kr. Nandi^b, Dip Jyoti Bora^c

^aDepartment of Mathematics, Gauhati University, Guwahati 781014, India

^bDepartment of Mathematics, Basugaon College, Basugaon-783372 Assam, India

^cDepartment of Mathematics, Cotton University, Guwahati 781001, India

*Corresponding Author e-mail: dssaikia18@gmail.com

Received May 11, 2024; revised July 7, 2024; accepted July 12, 2024

The current investigation aims at to examine the effect of radiation absorption, heat generation and Dufour number on MHD Casson fluid flow past an exponentially accelerated vertical plate in a porous medium with chemical reaction. The governing equations for momentum, energy and concentration are solved by implementing the Laplace transformation method. Skin friction, rate of heat transfer and rate of mass transfer expressions are also extracted and depicted in tabular form. Investigation simulates that Casson parameter diminished the fluid velocity, whereas energy flux due to a mass concentration gradient improves the temperature field of the flow problem. In addition to this, temperature field is observed to be developed under the influence of radiation absorption and heat generation. Furthermore, the effects of different non-dimensional parameters on velocity field, temperature fluid and species concentration are exhibited graphically.

Keywords: MHD; Radiation absorption; Casson fluid; Heat generation; Dufour effect

PACS: 44.25. f, 44.30. v, 44.40. a, 47.65. d

1. INTRODUCTION

Magnetohydrodynamics (MHD) has an extensive range of application in abundant areas of applied research such as engineering, astrophysics, biological science etc. Hannes Alfvén [1], the great plasma physicist, initiated the field of MHD. The influence of unsteady MHD natural convective flow in the vicinity of an impulsively moving upright plate was cogitated by Seth *et al.* [2]. BS Goud [3] studied the effects of heat radiation on the MHD stagnation point stream across a stretched sheet with slip boundary conditions. Rath *et al.* [4] probed at the effects of Dufour and viscous dissipation on MHD natural convective flow through an accelerated vertical plate. Singh *et al.* [5] investigated the effects of time-varying wall temperature and concentration on MHD free convective flow of a rotating fluid owing to moving free-stream with hall and ion-slip currents.

In recent times, due to the significant growth of technological industries, the importance of the out-turn of thermal radiation on MHD heat transfer problems is seen to be increasing. There are numerous engineering activities that takes place at a very high temperature and therefore to avoid radiation from such activities, knowledge of thermal radiation becomes more important to build suitable equipment. Through a vertically travelling absorbent plate, the effect of radiation absorption on MHD convective flow was studied by Krishna *et al.* [6]. Using radiation absorption effect Rao *et al.* [7] analyzed the unsteady MHD flow past an exponentially accelerated plate surrounded by porous medium. In addition, Endalew and Nayak [8] also studied the effects of thermal radiation and inclined magnetic field on MHD flow past a linearly accelerated plate in the existence of porous medium.

Fluids that defiant Newton's law of viscosity termed as non-Newtonian fluids. This means that in case of a non-Newtonian fluid constant viscosity becomes independent of time. The most common example of non-Newtonian fluids is honey, butter, blood, saliva, Casson fluid etc. Kateria and Patel [9] investigated the influence of heat generation and chemical reaction on MHD Casson fluid flow over an upright plate surrounded by porous medium. Zhou *et al.* [10] investigated the two-dimensional time dependent radiative Casson fluid flow under the impact of heat source. Some other researcher such as, Sulochana *et al.* [11], Reyaz *et al.* [12], also performed their research work related to MHD heat and mass transfer by using Casson fluid.

In many engineering applications, the influence of heat generation has been found to be of considerable importance. There are many researchers, in whose research work the application of the effect of heat generation is observed. Among them, Jamuna and Balla [13], Ali *et al.* [14], Khan *et al.* [15] are the researcher who have studied the impact heat generation in their research work. The impact of non-uniform heat source/sink and temperature dependent viscosity modeled by Reynolds on Cattaneo-Christov heat flow was studied by Nayak *et al.* [16].

The energy flux due to a mass concentration gradient is called Dufour effect. Nayak *et al.* [17] investigated the impacts of Dufour and Soret on unsteady MHD flow past a stretching upright plate in porous medium. In addition, the impact of Dufour effect can also be seen in many other studies by various researchers such as Ahammad and Krishna [18], Jawad *et al.* [19] etc.

In recent times, it is observed that the chemical reaction becomes an integrated part of the research work of various researcher due to the extensive application of chemical reaction in various mechanisms of chemical engineering and heat and mass transfer problems.

Most recently, in the research work of Ahmed and Saikia [20] was found to be use of chemical reaction to investigate the changes of various flow characteristics such as fluid concentration and fluid velocity etc. In presence of chemical reaction, the unsteady MHD natural convective flow past an exponentially accelerated plate embedded in a porous medium was investigated by Rath and Nayak [21]. Moreover, we may also cited the research work of the researchers – Gopal *et al.* [22], Raddy *et al.* [23], Haq *et al.* [24] for their excellent work using chemical reaction.

The preeminent objective of this research work is to figure out an analytical solution for the effects of radiation absorption, Dufour, heat generation and chemical reaction on MHD Casson fluid flow past an exponentially accelerated vertical plate in a porous medium with thermal and solutal ramped conditions. Kateria and Patel [25], Mopuri *et al.* [26], Reddy and Chamkha *et al.* [27] are some of the prominent researchers in whose work the effects of radiation absorption, chemical reactions, the Dufour effect, and heat generation and absorption can be seen. Although the use of all effects such as Dufour, radiation absorption, chemical reactions, and heat generation in the presence of Casson fluid distinguishes our study from others.

2. MATHEMATICAL FORMULATION

As depicted in Figure 1, a rectangular cartesian coordinate system is set up so that x' -axis is taken in upward vertical direction along which the length of the plate is measured.

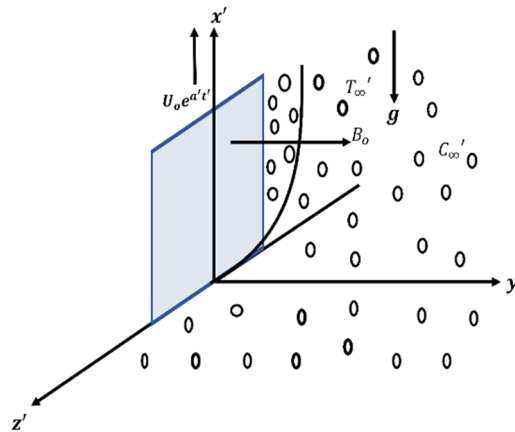


Figure 1. Physical outline of the flow problem

The y' -axis is taken parallel to the direction of the magnetic field and z' -axis is taken along the width of the plate. Now to idealize the flow problem the following assumptions are taken into account.

- Initially at $t' \leq 0$, the plate and the neighboring fluid are at static condition.
- The plate embedded in the porous medium maintain a uniform temperature T'_∞ .
- The fluid adjacent to the plate maintain a uniform concentration C'_∞ at each point of the fluid.
- The plate accelerated exponentially with velocity $U_0 e^{alpha t'}$ at time $t' > 0$ and at this period of time the concentration

and temperature of the fluid is either gets improved or dropped to $C' = C'_\infty + \frac{(C'_w - C'_\infty)t'}{t_0}$ and $T' = T'_\infty + \frac{(T'_w - T'_\infty)t'}{t_0}$ respectively.

- There is no external electric field present.
- The fluid considered to be non-Newtonian in nature.

Under the above assumptions the governing equations for the flow problem are sated below:

Equation of continuity:

$$\frac{\partial u'}{\partial x'} = 0 \tag{1}$$

Momentum equation:

$$\frac{\partial u'}{\partial t'} = \nu \left(1 + \frac{1}{\beta} \right) \frac{\partial^2 u'}{\partial y'^2} - \frac{\sigma B_0^2 u'}{\rho} + g \bar{\beta}' (C' - C'_\infty) + g \beta' (T' - T'_\infty) \tag{2}$$

Energy equation:

$$\frac{\partial T'}{\partial t'} = \frac{\kappa}{\rho C_p} \frac{\partial^2 T'}{\partial y'^2} + \frac{Q_o}{\rho C_p} (T' - T'_\infty) + Q_l (C' - C'_\infty) + \frac{D_M K_T}{C_s} \frac{\partial^2 C'}{\partial y'^2}. \tag{3}$$

Species continuity equation:

$$\frac{\partial C'}{\partial t'} = D_M \frac{\partial^2 C'}{\partial y'^2} - \bar{k}' (C' - C'_\infty). \tag{4}$$

Equation of state:

$$\rho_\infty = \rho \left[1 + \beta' (T' - T'_\infty) + \bar{\beta}' (C' - C'_\infty) \right] \tag{5}$$

The initially opted boundary conditions are:

$$\left. \begin{aligned} \text{At } y' \geq 0 : u' = 0, T' = T'_\infty, C' = C'_\infty; t' \leq 0, \\ u' = U_o e^{a't'}, T' = T'_M, C' = C'_M; 0 < t' \leq t_o \\ u' = U_o e^{a't'}, T' = T'_w, C' = C'_w; t' > t_o \end{aligned} \right\} \text{ at } y' = 0; \tag{6}$$

As $y' \rightarrow \infty : u' \rightarrow 0, T' \rightarrow T'_\infty, C' \rightarrow C'_\infty, \forall t' > 0$

where,

$$T'_M = T'_\infty + (T'_w - T'_\infty) \frac{t'}{t_o}, \quad C'_M = C'_\infty + (C'_w - C'_\infty) \frac{t'}{t_o}.$$

Introducing the non-dimensional parameters:

$$\left. \begin{aligned} y = \frac{U_o y'}{v}, t = \frac{t'}{t_o}, u = \frac{u'}{U_o}, T = \frac{T' - T'_\infty}{T'_w - T'_\infty}, C = \frac{C' - C'_\infty}{C'_w - C'_\infty}, Gr = \frac{v g \beta' (T'_w - T'_\infty)}{U_o^3}, \\ Gm = \frac{v g \bar{\beta}' (C'_w - C'_\infty)}{U_o^3}, M = \frac{\sigma B_o^2 v}{\rho U_o^2}, H = \frac{Q_o v}{\rho C_p U_o^2}, K = \frac{K' U_o^2}{v^2}, a = a' t_o, \\ Q_l^* = \frac{Q_l (C'_w - C'_\infty) t_o}{T'_w - T'_\infty}, Pr = \frac{v \rho C_p}{\kappa}, Du = \frac{D_M K_T (C'_w - C'_\infty)}{C_s v (T'_w - T'_\infty)}, Ra = \frac{U_o^2 t_o}{v}, \\ k = \bar{k}' t_o, Sc = \frac{v}{D_M}. \end{aligned} \right\}$$

Implementing the non-dimensional parameters, the governing equations (2), (4), (5) and the initial boundary condition (6) transform to the following structures:

$$\frac{\partial C}{\partial t} = \frac{Ra}{Sc} \frac{\partial^2 C}{\partial y^2} - kC. \tag{7}$$

$$\frac{\partial T}{\partial t} = \frac{Ra}{Pr} \frac{\partial^2 T}{\partial y^2} + H Ra T + Q_l^* C + Du Ra \frac{\partial^2 C}{\partial y^2}. \tag{8}$$

$$\frac{\partial u}{\partial t} = Ra \left(1 + \frac{1}{\beta} \right) \frac{\partial^2 u}{\partial y^2} - Ra \left(M + \frac{1}{K} \right) u + Ra Gr T + Ra Gc Gm. \tag{9}$$

$$\left. \begin{aligned} \text{At } y \geq 0 : u = 0, C = 0, T = 0; t \leq 0, \\ \text{At } y = 0 : \begin{cases} u = e^{at}, T = t, C = t; & 0 < t \leq 1 \\ u = e^{at}, T = 1, C = 1; & T > 1 \end{cases} \\ \text{As } y \rightarrow \infty : u \rightarrow 0, C \rightarrow 0, T \rightarrow 0, \forall t > 0. \end{aligned} \right\} \tag{10}$$

4. METHOD OF SOLUTION

We have implemented the Laplace transformation method to find an analytical solution for concentration, temperature, and velocity field for the flow problem. The procedure for accomplishing these solutions is stated below: Taking Laplace transformation of the equations (7)-(9) gives:

$$Ra \frac{d^2 \bar{C}}{dy^2} - Sc(s+k)\bar{C} = 0, \tag{11}$$

$$\frac{Ra}{Pr} \frac{d^2 \bar{T}}{dy^2} + (H Ra - s)\bar{T} = -Q_l^* \bar{C} - Du Ra \frac{d^2 \bar{C}}{dy^2}, \tag{12}$$

$$Ra \left(1 + \frac{1}{\beta} \right) \frac{d^2 \bar{u}}{dy^2} - (s + I) \bar{u} = -Ra Gr \bar{T} - Ra Gm \bar{C}, \tag{13}$$

Again, taking Laplace transformation of the non-dimensional initial boundary condition stated in (10) gives:

$$At \ y = 0: \left. \begin{aligned} \bar{T} &= \frac{1}{s^2} (1 - e^{-s}), \bar{C} = \frac{1}{s^2} (1 - e^{-s}), \bar{u} = \frac{1}{s - a} \\ As \ y \rightarrow \infty: \bar{T} &\rightarrow 0, \bar{C} \rightarrow 0, \bar{u} \rightarrow 0 \end{aligned} \right\} \tag{14}$$

The equations (11) - (13) are solved subject to the condition (14) and the solutions are obtained as follows:

$$\bar{C} = \frac{1 - e^{-s}}{s^2} e^{-\sqrt{\lambda_4} \sqrt{s+k} y}. \tag{15}$$

$$\begin{aligned} \bar{T} &= \frac{1 - e^{-s}}{s^2} e^{-\sqrt{s+E} \sqrt{\lambda_2} y} + \lambda_4 \frac{1 - e^{-s}}{s^2} \frac{e^{-\sqrt{s+E} \sqrt{\lambda_2} y}}{s + \lambda_5} + \lambda_6 \frac{1 - e^{-s}}{s^2} \frac{s+k}{s + \lambda_5} e^{-\sqrt{s+E} \sqrt{\lambda_2} y} \\ &\quad - \lambda_4 \frac{1 - e^{-s}}{s^2} \frac{e^{-\sqrt{s+k} \sqrt{\lambda_4} y}}{s + \lambda_5} - \lambda_6 \frac{1 - e^{-s}}{s^2} \frac{s+k}{s + \lambda_5} e^{-\sqrt{s+k} \sqrt{\lambda_4} y}, \end{aligned} \tag{16}$$

$$\begin{aligned} \bar{u} &= \frac{1}{s - a} e^{-\sqrt{s+I} \sqrt{\delta} y} - \frac{\lambda_6 (1 - e^{-s})}{s^2 (s + \lambda_7)} e^{-\sqrt{s+I} \sqrt{\delta} y} - \frac{\lambda_6 \lambda_3 (1 - e^{-s})}{s^2 (s + \lambda_7)(s + \lambda_4)} e^{-\sqrt{s+I} \sqrt{\delta} y} \\ &\quad - \frac{\lambda_6 \lambda_5 (1 - e^{-s})(s+k)}{s^2 (s + \lambda_7)(s + \lambda_4)} e^{-\sqrt{s+I} \sqrt{\delta} y} - \frac{\lambda_8 \lambda_3 (1 - e^{-s})}{s^2 (s + \lambda_9)(s + \lambda_4)} e^{-\sqrt{s+I} \sqrt{\delta} y} - \frac{\lambda_8 \lambda_5 (1 - e^{-s})(s+k)}{s^2 (s + \lambda_4)(s + \lambda_9)} e^{-\sqrt{s+I} \sqrt{\delta} y} \\ &\quad - \frac{\lambda_{10} (1 - e^{-s})}{s^2 (s + \lambda_9)} e^{-\sqrt{s+I} \sqrt{\delta} y} + \frac{\lambda_6 (1 - e^{-s})}{s^2 (s + \lambda_7)} e^{-\sqrt{s+E} \sqrt{\lambda_2} y} + \frac{\lambda_6 \lambda_3 (1 - e^{-s})}{s^2 (s + \lambda_7)(s + \lambda_4)} e^{-\sqrt{s+E} \sqrt{\lambda_2} y} \\ &\quad + \frac{\lambda_6 \lambda_5 (1 - e^{-s})(s+k)}{s^2 (s + \lambda_7)(s + \lambda_4)} e^{-\sqrt{s+E} \sqrt{\lambda_2} y} + \frac{\lambda_8 \lambda_3 (1 - e^{-s})}{s^2 (s + \lambda_9)(s + \lambda_4)} e^{-\sqrt{s+k} \sqrt{\lambda_4} y} + \frac{\lambda_8 \lambda_5 (1 - e^{-s})(s+k)}{s^2 (s + \lambda_4)(s + \lambda_9)} e^{-\sqrt{s+k} \sqrt{\lambda_4} y} \\ &\quad + \frac{\lambda_{10} (1 - e^{-s})}{s^2 (s + \lambda_9)} e^{-\sqrt{s+k} \sqrt{\lambda_4} y}, \end{aligned} \tag{17}$$

where,

$$\delta = \frac{1}{\left(1 + \frac{1}{\beta} \right) Ra}, \quad \lambda_1 = \frac{Sc}{Ra}, \quad I = \left(M + \frac{1}{K} \right) Ra,$$

$$\lambda_2 = \frac{Pr}{Ra}, \quad \lambda_3 = \frac{\lambda_1}{\lambda_2}, \quad \lambda_4 = \frac{Q_l^*}{\lambda_3 - 1},$$

$$\lambda_5 = \frac{\lambda_3 k - E}{\lambda_3 - 1}, \quad E = -H Ra, \quad \lambda_6 = \frac{\lambda_1 Du Ra}{\lambda_3 - 1},$$

$$\lambda_7 = \frac{-Ra Gr}{\delta \lambda_2 - 1}, \quad \lambda_8 = \frac{\delta E \lambda_2 - I}{\delta \lambda_2 - 1}, \quad \lambda_9 = \frac{Ra Gr}{\delta \lambda_1 - 1},$$

$$\lambda_{10} = \frac{\delta k \lambda_1 - I}{\delta \lambda_1 - 1}, \quad \lambda_{11} = -\frac{Ra Gm}{\delta \lambda_1 - 1}, \quad Z_1 = -\frac{1}{\lambda_8^2},$$

$$Z_2 = \frac{1}{\lambda_8}, \quad Z_3 = \frac{1}{\lambda_8^2}, \quad J_1 = \frac{\lambda_5 + \lambda_8}{\lambda_5^2 \lambda_8^2},$$

$$J_2 = \frac{1}{\lambda_5 \lambda_8}, \quad J_3 = -\frac{1}{\lambda_5^2 (\lambda_5 - \lambda_8)}, \quad J_4 = \frac{1}{\lambda_8^2 (\lambda_5 - \lambda_8)},$$

$$L_1 = \frac{\lambda_5 \lambda_8 - k (\lambda_5 + \lambda_8)}{\lambda_5^2 \lambda_8^2}, \quad L_2 = \frac{k}{\lambda_5 \lambda_8}, \quad L_3 = \frac{\lambda_5 - k}{\lambda_5^2 (\lambda_5 - \lambda_8)}, \quad L_4 = \frac{k - \lambda_8}{\lambda_8^2 (\lambda_5 - \lambda_8)}, \quad F_1 = -\frac{(\lambda_5 + \lambda_{10})}{\lambda_5^2 \lambda_{10}^2}.$$

Finally, the following solutions for temperature profile, concentration profile and velocity profile are attained on picking inverse Laplace transformation of Equations (15)-(17):

$$C = f_1 - \bar{f}_1 \tag{18}$$

where,

$$f_1 = f(\lambda_1, k, y, t), \quad \bar{f}_1 = f(\lambda_1, k, y, t-1)H.$$

$$\begin{aligned} T &= (\lambda_4 A_2 + \lambda_6 B_2)(f_1 - \bar{f}_1) + (1 + \lambda_4 A_2 + \lambda_6 B_2)(h_2 - \bar{h}_2) \\ &+ (\lambda_4 A_1 + \lambda_6 B_1)(\psi_1 - \bar{\psi}_1) + (\lambda_4 A_3 + \lambda_6 B_3)(\psi_2 - \bar{\psi}_2) \\ &+ (\lambda_4 A_1 + \lambda_6 B_1)(\psi_3 - \bar{\psi}_3) + (\lambda_4 A_3 + \lambda_6 B_3)(\psi_4 - \bar{\psi}_4). \end{aligned} \tag{19}$$

where,

$$\begin{aligned} f_1 &= f(\lambda_1, k, y, t) & \bar{f}_1 &= f(\lambda_1, k, y, t-1)H \\ f_2 &= f(\lambda_2, \beta, y, t) & \bar{f}_2 &= f(\lambda_2, \beta, y, t-1)H \\ \psi_1 &= \psi(\lambda_2, \beta, y, t) & \bar{\psi}_1 &= \psi(\lambda_2, \beta, y, t-1)H \\ \psi_2 &= e^{-\lambda_5 t} \psi(\lambda_2, \beta - \lambda_5, y, t) \\ \bar{\psi}_2 &= e^{-\lambda_5(t-1)} \psi(\lambda_2, \beta - \lambda_5, y, t-1)H \\ \psi_3 &= \psi(\lambda_1, k, y, t) & \bar{\psi}_3 &= \psi(\lambda_1, k, y, t-1)H \\ \psi_4 &= e^{-\lambda_5 t} \psi(\lambda_1, k - \lambda_5, y, t) \\ \bar{\psi}_4 &= e^{-\lambda_5(t-1)} \psi(\lambda_1, k - \lambda_5, y, t-1)H. \end{aligned}$$

$$\begin{aligned} u &= G + R_1 \{(\psi_1 - \bar{\psi}_1) - (\psi_5 - \bar{\psi}_5)\} + R_2 \{(\psi_2 - \bar{\psi}_2) - (\psi_7 - \bar{\psi}_7)\} \\ &+ R_3 \{(\psi_3 - \bar{\psi}_3) - (\psi_5 - \bar{\psi}_5)\} + R_4 \{(\psi_4 - \bar{\psi}_4) - (\psi_7 - \bar{\psi}_7)\} \\ &+ R_5 \{(\psi_9 - \bar{\psi}_9) - (\psi_6 - \bar{\psi}_6)\} + R_6 \{(\psi_{10} - \bar{\psi}_{10}) - (\psi_8 - \bar{\psi}_8)\} \\ &+ R_7 \{(f_1 - \bar{f}_1) - (f_3 - \bar{f}_3)\} + R_8 \{(f_2 - \bar{f}_2) - (f_3 - \bar{f}_3)\}. \end{aligned} \tag{20}$$

where,

$$\begin{aligned} f_3 &= f(\delta, I, y, t), & \bar{f}_3 &= f(\delta, I, y, t-1)H, \\ \psi_5 &= \psi(\delta, I, y, t), & \bar{\psi}_5 &= \psi(\delta, I, y, t-1)H \\ \psi_7 &= e^{-\lambda_8 t} \psi(\delta, I - \lambda_8, y, t), \\ \bar{\psi}_7 &= e^{-\lambda_8(t-1)} \psi(\delta, I - \lambda_8, y, t-1)H, \\ \psi_8 &= e^{-\lambda_{10} t} \psi(\delta, I - \lambda_{10}, y, t), & \bar{\psi}_8 &= e^{-\lambda_{10}(t-1)} \psi(\delta, I - \lambda_{10}, y, t-1)H, \\ \psi_9 &= e^{-\lambda_8 t} \psi(\lambda_2, \beta - \lambda_8, y, t), & \bar{\psi}_9 &= e^{-\lambda_8(t-1)} \psi(\lambda_2, \beta - \lambda_8, y, t-1)H, \\ \psi_{10} &= e^{-\lambda_{10} t} \psi(\lambda_1, k - \lambda_{10}, y, t), & \bar{\psi}_{10} &= e^{-\lambda_{10}(t-1)} \psi(\lambda_1, k - \lambda_{10}, y, t-1)H. \end{aligned}$$

5. SKIN FRICTION

According to Newton's law of viscosity, the viscous drag per unit area at the plate is computed as follows:

$$\tau' = -\mu \left. \frac{\partial u'}{\partial y'} \right]_{y=0} = -\mu U_o \frac{\partial u}{\partial y} \frac{\partial y}{\partial y'} = -\mu U_o \frac{\partial u}{\partial y} \frac{\partial}{\partial y'} \left(\frac{U_o y'}{\nu} \right) = -\frac{\mu U_o^2}{\nu} \frac{\partial u}{\partial y}$$

The coefficient of skin friction at the plate is defined as

$$\tau = \left. \frac{\tau'}{\mu U_o^2} = -\frac{\partial u}{\partial y} \right]_{y=0}$$

$$\begin{aligned} \tau = & -G - R_1 \{(\Upsilon_1 - \bar{\Upsilon}_1) - (\Upsilon_5 - \bar{\Upsilon}_5)\} - R_2 \{(\Upsilon_2 - \bar{\Upsilon}_2) - (\Upsilon_7 - \bar{\Upsilon}_7)\} \\ & - R_3 \{(\Upsilon_3 - \bar{\Upsilon}_3) - (\Upsilon_5 - \bar{\Upsilon}_5)\} - R_4 \{(\Upsilon_4 - \bar{\Upsilon}_4) - (\Upsilon_7 - \bar{\Upsilon}_7)\} \\ & - R_5 \{(\Upsilon_9 - \bar{\Upsilon}_9) - (\Upsilon_6 - \bar{\Upsilon}_6)\} - R_6 \{(\Upsilon_{10} - \bar{\Upsilon}_{10}) - (\Upsilon_8 - \bar{\Upsilon}_8)\} \\ & - R_7 \{(\xi_1 - \bar{\xi}_1) - (\xi_3 - \bar{\xi}_3)\} - R_8 \{(\xi_2 - \bar{\xi}_2) - (\xi_3 - \bar{\xi}_3)\}. \end{aligned} \tag{21}$$

where,

$$\begin{aligned} \Upsilon_1 &= \left. \frac{\partial \psi_1}{\partial y} \right|_{y=0} = \Upsilon(\lambda_2, \beta, t), \quad \bar{\Upsilon}_1 = \left. \frac{\partial \bar{\psi}_1}{\partial y} \right|_{y=0} = \Upsilon(\lambda_2, \beta, t-1)H, \\ \Upsilon_2 &= \left. \frac{\partial \psi_2}{\partial y} \right|_{y=0} = e^{-\lambda_5 t} \Upsilon(\lambda_2, \beta - \lambda_5, t), \quad \bar{\Upsilon}_2 = \left. \frac{\partial \bar{\psi}_2}{\partial y} \right|_{y=0} = e^{-\lambda_5(t-1)} \Upsilon(\lambda_2, \beta - \lambda_5, t-1)H, \\ \Upsilon_3 &= \left. \frac{\partial \psi_3}{\partial y} \right|_{y=0} = \Upsilon(\lambda_1, k, t), \quad \bar{\Upsilon}_3 = \left. \frac{\partial \bar{\psi}_3}{\partial y} \right|_{y=0} = \Upsilon(\lambda_1, k, t-1)H, \\ \Upsilon_4 &= \left. \frac{\partial \psi_4}{\partial y} \right|_{y=0} = e^{-\lambda_5 t} \Upsilon(\lambda_1, k - \lambda_5, t), \quad \bar{\Upsilon}_4 = \left. \frac{\partial \bar{\psi}_4}{\partial y} \right|_{y=0} = e^{-\lambda_5(t-1)} \Upsilon(\lambda_1, k - \lambda_5, t-1)H, \\ \Upsilon_5 &= \left. \frac{\partial \psi_5}{\partial y} \right|_{y=0} = \Upsilon(\delta, I, t), \quad \bar{\Upsilon}_5 = \left. \frac{\partial \bar{\psi}_5}{\partial y} \right|_{y=0} = \Upsilon(\delta, I, t-1)H, \\ \Upsilon_6 &= \left. \frac{\partial \psi_6}{\partial y} \right|_{y=0} = e^{-\lambda_8 t} \Upsilon(\delta, I - \lambda_8, t), \quad \bar{\Upsilon}_6 = \left. \frac{\partial \bar{\psi}_6}{\partial y} \right|_{y=0} = e^{-\lambda_8(t-1)} \Upsilon(\delta, I - \lambda_8, t-1)H, \\ \Upsilon_7 &= \left. \frac{\partial \psi_7}{\partial y} \right|_{y=0} = e^{-\lambda_5 t} \Upsilon(\delta, I - \lambda_5, t), \quad \bar{\Upsilon}_7 = \left. \frac{\partial \bar{\psi}_7}{\partial y} \right|_{y=0} = e^{-\lambda_5(t-1)} \Upsilon(\delta, I - \lambda_5, t-1)H, \\ \Upsilon_8 &= \left. \frac{\partial \psi_8}{\partial y} \right|_{y=0} = e^{-\lambda_{10} t} \Upsilon(\delta, I - \lambda_{10}, t), \quad \bar{\Upsilon}_8 = \left. \frac{\partial \bar{\psi}_8}{\partial y} \right|_{y=0} = e^{-\lambda_{10}(t-1)} \Upsilon(\delta, I - \lambda_{10}, t-1)H, \\ \Upsilon_9 &= \left. \frac{\partial \psi_9}{\partial y} \right|_{y=0} = e^{-\lambda_8 t} \Upsilon(\lambda_2, \beta - \lambda_8, t), \quad \bar{\Upsilon}_9 = \left. \frac{\partial \bar{\psi}_9}{\partial y} \right|_{y=0} = e^{-\lambda_8(t-1)} \Upsilon(\lambda_2, \beta - \lambda_8, t-1)H, \\ \Upsilon_{10} &= \left. \frac{\partial \psi_{10}}{\partial y} \right|_{y=0} = e^{-\lambda_{10} t} \Upsilon(\lambda_1, k - \lambda_{10}, t), \quad \bar{\Upsilon}_{10} = \left. \frac{\partial \bar{\psi}_{10}}{\partial y} \right|_{y=0} = e^{-\lambda_{10}(t-1)} \Upsilon(\lambda_1, k - \lambda_{10}, t-1)H, \\ V(\delta, I, a, t) &= \left. \frac{\partial G}{\partial y} \right|_{y=0}. \end{aligned}$$

6. SHERWOOD NUMBER

The calculation of the Sherwood number relies on Fick's law of diffusion and is connected with the rate of mass transfer at the plate.

The mass flux M_w from the plate at $y'=0$ can be obtained using the following method:

$$M_w = -D_M \left. \frac{\partial C'}{\partial y'} \right|_{y'=0} = -\frac{D_M U_o (C'_w - C'_\infty)}{\nu} \left. \frac{\partial C}{\partial y} \right|_{y=0},$$

Thus, the coefficient of rate of mass transport at the plate is,

$$\begin{aligned} Sh &= \frac{M_w}{D_M U_o (C'_w - C'_\infty)} = -\left. \frac{\partial C}{\partial z} \right|_{z=0}, \\ Sh &= -\left. \frac{\partial C}{\partial y} \right|_{y=0} = -(\xi_1 - \bar{\xi}_1). \end{aligned} \tag{22}$$

where,

$$\xi_1 = \left. \frac{\partial h_1}{\partial y} \right|_{y=0} = \xi(\lambda_1, k, t) \text{ and}$$

$$\bar{\xi}_1 = \left. \frac{\partial \bar{h}_1}{\partial y} \right|_{y=0} = \xi(\lambda_1, k, t-1)H.$$

7. NUSSELT NUMBER

The Nusselt number, which is the ratio of convective to conductive thermal transfer in the fluid across the boundary, is computed by Fourier’s conduction law to estimate and comprehend the rate of heat transfer at the plate. The heat flux Q' from the plate $y' = 0$ to the fluid defined by the Fourier’s law of conduction can be obtained by

$$Q' = -\kappa \left. \frac{\partial T'}{\partial y'} \right|_{y'=0} = -\frac{\kappa U_o (T'_w - T'_\infty)}{\nu} \left. \frac{\partial T}{\partial y} \right|_{y=0},$$

The coefficient of rate of heat transfer at the plate is,

$$Nu = \frac{\nu Q'}{\kappa U_o (T'_w - T'_\infty)} = -\left. \frac{\partial T}{\partial y} \right|_{y=0},$$

$$Nu = -(\lambda_4 A_2 + \lambda_6 B_2)(\xi_1 - \bar{\xi}_1) - (1 + \lambda_4 A_2 + \lambda_6 B_2)(\xi_2 - \bar{\xi}_2) - (\lambda_4 A_1 + \lambda_6 B_1)(Y_1 - \bar{Y}_1) - (\lambda_4 A_3 + \lambda_6 B_3)(Y_2 - \bar{Y}_2) - (\lambda_4 A_1 + \lambda_6 B_1)(Y_3 - \bar{Y}_3) - (\lambda_4 A_3 + \lambda_6 B_3)(Y_4 - \bar{Y}_4). \tag{23}$$

8. RESULTS AND DISCUSSIONS

In the present investigation it was explored that the impact of Casson parameter (β) reduced the fluid velocity, which is reflected in Figure 2 Moreover, the Casson parameter was found to reduce the momentum boundary layer thickness. Figure 3 exhibits that the fluid motion gets accelerated due to the enhancement of solutal Grashof number (Gm). In other words, it can be said that the fluid velocity upsurges due to the thermal buoyancy force. Further this figure indicates that the fluid velocity first boosts in a very thin layer proximate to the plate and after achieving a peak value it drops down to it’s minimum value. This is due to the bouyancy force being more effective in the vicinity of the plate. In addition, this figure demonstrates that the effect of buoyancy force on velocity gets disappeared at the free stream.

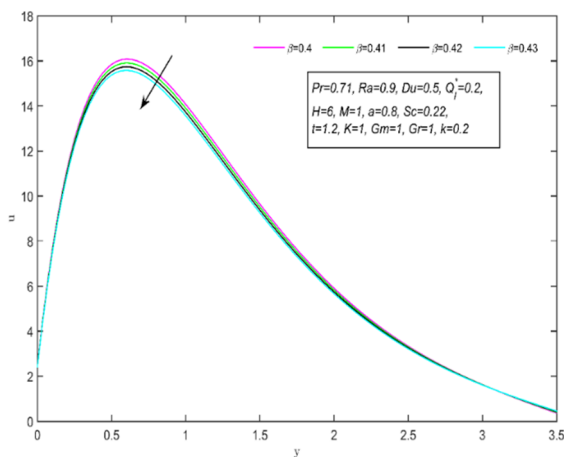


Figure 2. Velocity versus distinct β

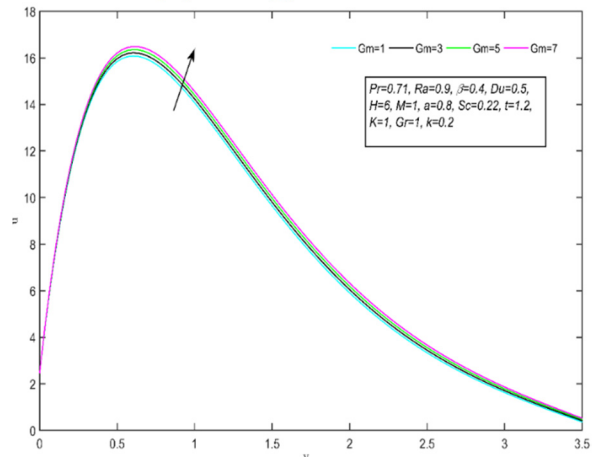


Figure 3. Velocity versus distinct Gm

As illustrated in Figure 3, Figure 4 depicts that, the thermal Grashof number (Gr) also controls fluid velocity similarly to the solutal Grashof number. Both the figures, i.e Figure 3 and Figure 4 uniquely established the fact that the fluid velocity initially escalates in a very thin layer proximate to the plate and after reaching it’s peak value, it asymptotically drops down to its minimum value $u=0$ at $y \rightarrow \infty$. From Figure 5 it is evident that the increment of magnetic parameter (M) rises the fluid velocity. This is due to the fact that the applied magnetic field produce a force called Lorentz force, which resist the fluid motion.

Figure 6 reveals that the heat generation parameter enhanced the fluid motion. This discloses the physical reality that, as heat generation increases, the temperature of the fluid flow improves and which in turn accelerated the fluid

motion. Figure 7-8 demonstrate the variation of temperature field versus normal co-ordinate y for isothermal and ramped plate condition. In both the figures it is clear that, as the heat generation parameter (H) increases, the temperature of the fluid flow improves. Obviously, this is in accordance with the physical reality that as the heat generation of the source increases, the temperature of the surrounding medium improves due to conduction phenomena.

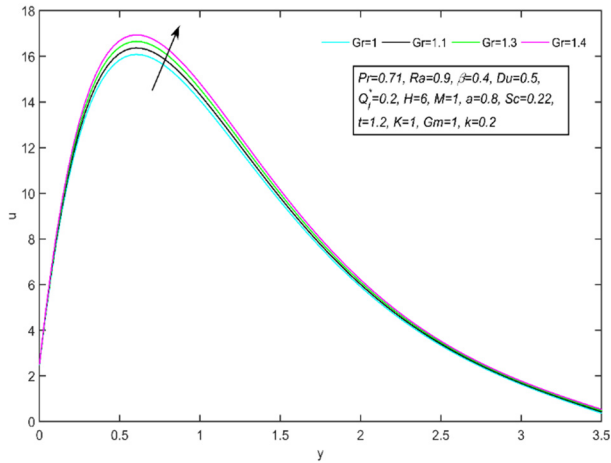


Figure 4. Velocity versus distinct Gr

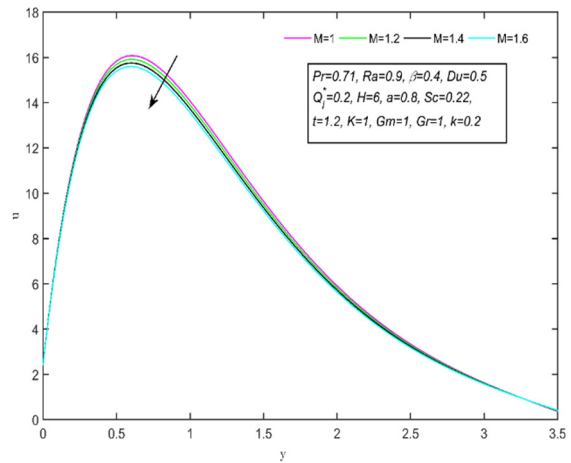


Figure 5. Velocity versus distinct M

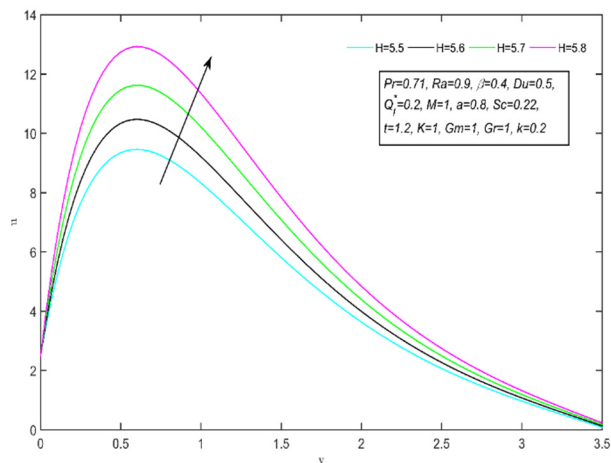


Figure 6. Velocity versus distinct H

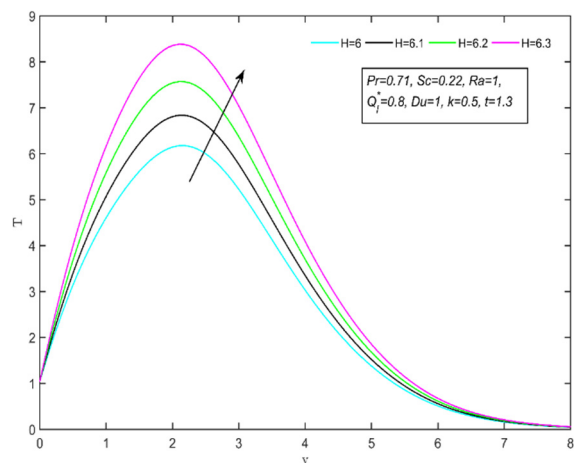


Figure 7. Temperature versus distinct H

Figure 9-10 shows that improving the radiation absorption parameter (Q_t^*) boosts the flow field temperature under both isothermal and ramped plate conditions. The larger the value of the radiation absorption parameter, which implies a significant increase in the dominance of conduction over absorption radiation, resulting in an increase in the buoyancy force and thickness of the thermal and momentum boundary layers.

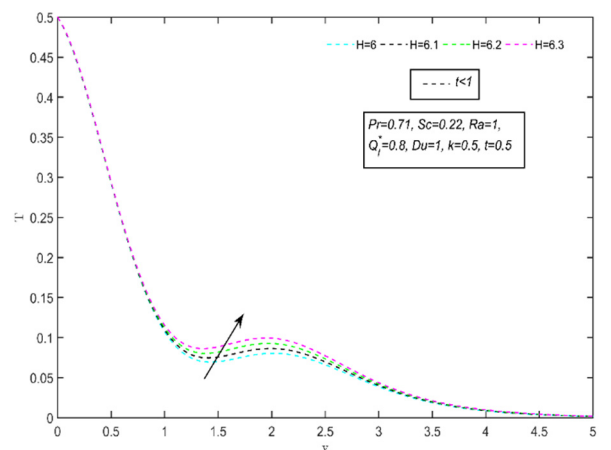


Figure 8. Temperature versus distinct H for $t < 1$

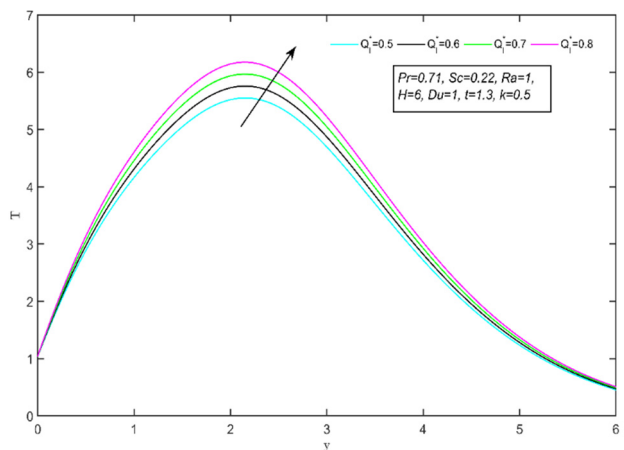


Figure 9. Temperature versus distinct Q_t^*

The diffusion thermal effect (Du) has a great influence on temperature field. Figure 11-12 reflects this impact of thermal diffusion on temperature field and due to which enlargement of temperature field occurs in both the isothermal and ramped plate conditions. Figure 13-14 establishes the relationship between concentration field versus chemical reaction parameter k . In both the figures the concentration of the fluid seen to be improved. Physically it divulges the fact that as the consumption of species increases, the fluid becomes thicker and as a result concentration of the fluid drops. In Figure 15-16, it is noticed that as the ramped parameter (Ra) increases, the fluid concentration hikes. This implies the fact that the ramped parameter has a tendency to increase fluid concentration.

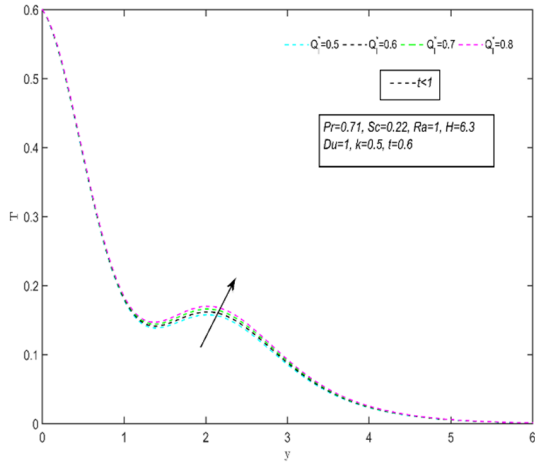


Figure 10. Temperature versus distinct Q_i^* for $t < 1$

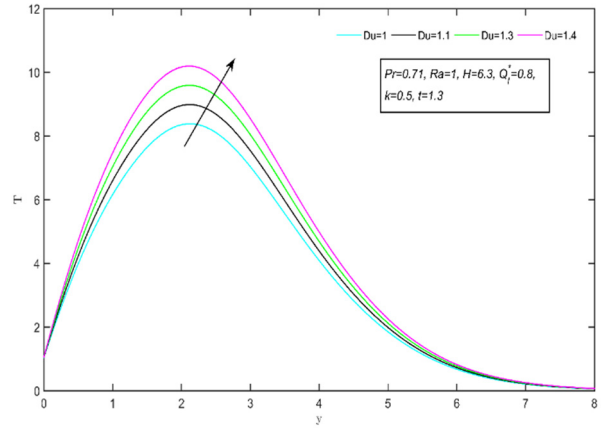


Figure 11. Temperature versus distinct Du

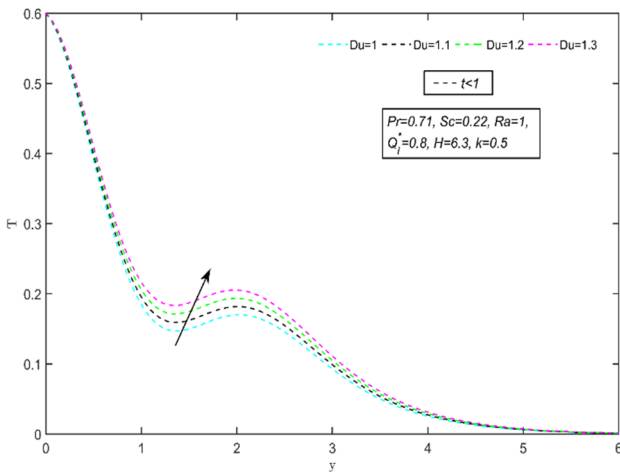


Figure 12. Temperature versus distinct Du for $t < 1$

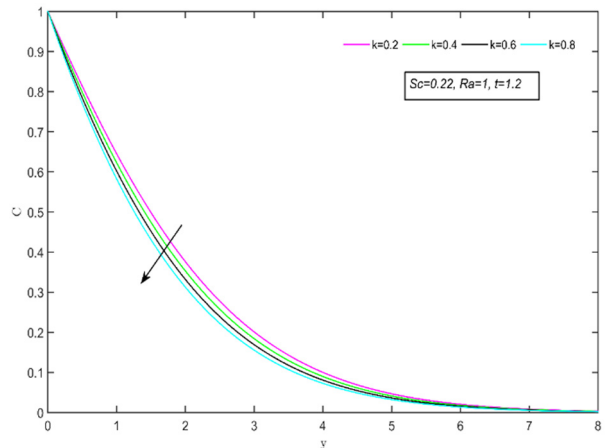


Figure 13. Concentration versus distinct k

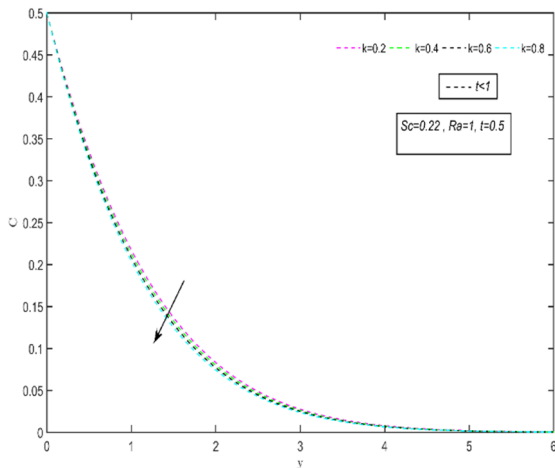


Figure 14. Concentration versus distinct k for $t < 1$

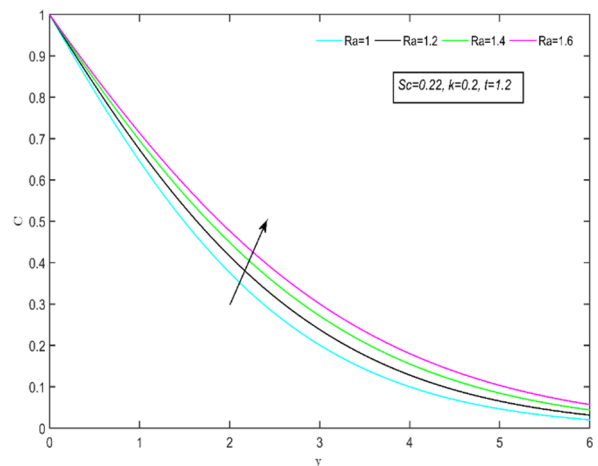


Figure 15. Concentration versus distinct Ra

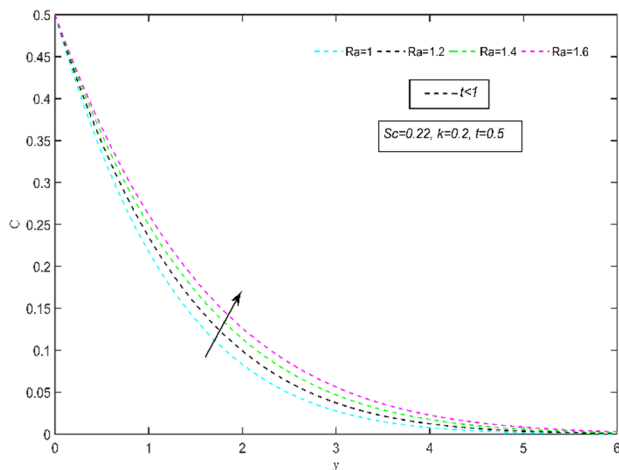


Figure 16. Concentration versus distinct Ra for $t < 1$

The variation of skin friction, Nusselt number and Sherwood number for different non dimensional parameters is shown in Table 1, Table 2 and Table 3 respectively. We have also made a comparison between the present study and an earlier study by Kateria and Patel to validate our findings. From Table 1, it is found that the increment of the non-dimensional parameters Pr , Sc , Gm , k , K , H , t , Q_l^* , Du hikes the frictional drag (τ). Moreover, the enhancement of the non-dimensional parameters β , Gr , M diminished the frictional resistance of the fluid flow.

Table 1. Variation of Skin friction

Pr	β	Sc	Gr	Gm	k	M	K	H	t	Q_l^*	Ra	a	Du	Value of skin friction (τ)
2	0.5	0.66	8	5	0.5	1	6	3	1.2	0.4	0.5	0.4	0.5	7.9037
3	0.5	0.66	8	5	0.5	1	6	3	1.2	0.4	0.5	0.4	0.5	11.1574
2	0.6	0.66	8	5	0.5	1	6	3	1.2	0.4	0.5	0.4	0.5	7.1107
2	0.7	0.66	8	5	0.5	1	6	3	1.2	0.4	0.5	0.4	0.5	6.4600
2	0.5	0.68	8	5	0.5	1	6	3	1.2	0.4	0.5	0.4	0.5	8.2617
2	0.5	0.7	8	5	0.5	1	6	3	1.2	0.4	0.5	0.4	0.5	8.6495
2	0.5	0.66	8.2	5	0.5	1	6	3	1.2	0.4	0.5	0.4	0.5	7.7897
2	0.5	0.66	8.4	5	0.5	1	6	3	1.2	0.4	0.5	0.4	0.5	7.6758
2	0.5	0.66	8	5.2	0.5	1	6	3	1.2	0.4	0.5	0.4	0.5	7.9313
2	0.5	0.66	8	5.4	0.5	1	6	3	1.2	0.4	0.5	0.4	0.5	7.9588
2	0.5	0.66	8	5	0.6	1	6	3	1.2	0.4	0.5	0.4	0.5	8.1796
2	0.5	0.66	8	5	0.7	1	6	3	1.2	0.4	0.5	0.4	0.5	8.4597
2	0.5	0.66	8	5	0.5	2	6	3	1.2	0.4	0.5	0.4	0.5	7.3393
2	0.5	0.66	8	5	0.5	3	6	3	1.2	0.4	0.5	0.4	0.5	6.8698
2	0.5	0.66	8	5	0.5	1	7	3	1.2	0.4	0.5	0.4	0.5	7.9184
2	0.5	0.66	8	5	0.5	1	8	3	1.2	0.4	0.5	0.4	0.5	7.9294
2	0.5	0.66	8	5	0.5	1	6	3.2	1.2	0.4	0.5	0.4	0.5	8.6267
2	0.5	0.66	8	5	0.5	1	6	3.4	1.2	0.4	0.5	0.4	0.5	9.4493
2	0.5	0.66	8	5	0.5	1	6	3	1.3	0.4	0.5	0.4	0.5	10.2623
2	0.5	0.66	8	5	0.5	1	6	3	1.4	0.4	0.5	0.4	0.5	13.2560
2	0.5	0.66	8	5	0.5	1	6	3	1.2	0.5	0.5	0.4	0.5	8.4221
2	0.5	0.66	8	5	0.5	1	6	3	1.2	0.6	0.5	0.4	0.5	8.9404
2	0.5	0.66	8	5	0.5	1	6	3	1.2	0.4	0.5	0.4	0.6	8.9032
2	0.5	0.66	8	5	0.5	1	6	3	1.2	0.4	0.5	0.4	0.7	9.9026

Table 2 depicts that as the value of the non-dimensional parameters H , t , Q_l^* , Du increases, the rate of heat transfer declines. On the other hand, the increment of the Prandtl number Pr improves the rate of heat transfer. Table 3 shows that the escalating values of the non-dimensional parameters k , Sc , Ra increases the Sherwood number which is associated with rate of mass transfer of the fluid flow.

Table 2. Variation of Nusselt number (Nu)

Pr	H	t	Q_l^*	Du	Value of Nusselt number
2	3	1.2	0.4	0.5	-14.1252
3	3	1.2	0.4	0.5	-1.8467
2	3.2	1.2	0.4	0.5	-16.3795
2	3.4	1.2	0.4	0.5	-19.0530
2	3	1.3	0.4	0.5	-19.2844

Pr	H	t	Q_i^*	Du	Value of Nusselt number
2	3	1.4	0.4	0.5	-26.0778
2	3	1.2	0.5	0.5	-15.3553
2	3	1.2	0.6	0.5	-16.5854
2	3	1.2	0.4	0.6	-17.3255
2	3	1.2	0.4	0.7	-20.5258

Table 3. Comparison of Sherwood number values obtained by Kateria and Patel and the current authors

k	Sc	t	Kateria and Patel [8] (Sh)	Ra	Newly finding values of Sherwood number (Sh)	Ra	Newly finding values of Sherwood number (Sh)
5	0.66	0.4	0.9062	1.1	0.8640	1	0.9062
5.1	0.66	0.4	0.9118	1.1	0.8693	1	0.9118
5.2	0.66	0.4	0.9173	1.1	0.8746	1	0.9173
5	0.7	0.4	0.9333	1.1	0.8898	1	0.9333
5	0.8	0.4	0.9977	1.1	0.9513	1	0.9977
5	0.66	0.5	1.0889	1.1	1.0383	1	1.0899
5	0.66	0.6	1.2711	1.1	1.2119	1	1.2711

9. COMPARISION OF FINDINGS

In order to validate our findings, we have made a comparison between our current findings of Sherwood number values incorporated with different non-dimensional parameters and the tabulated values for Sherwood number obtained by Kateria and Patel [8] in their research work. Comparing the current values of the Sherwood number with the previously investigated values obtained by Kateria and Patel, we see that when we set the ramped parameter to 1, the previous and current values of the Sherwood number are found identical.

10. CONCLUSIONS

The preeminent findings of this research work are enlisted below:

- The fluid velocity found to be improved asymptotically under the influence of heat generation parameter H , solutal Grashof number Gm , and thermal Grashof number Gr :
- In both the isothermal and ramped plate conditions, the temperature of the flow field spotted to be get enhanced under the influenced heat generation parameter H , radiation absorption parameter Q_i^* , and Dufour effect Du .
- The species concentration seen to be reduced under the influenced of chemical reaction parameter k in both the isothermal and ramped plate conditions. Moreover, it is evident that, in both the isothermal and ramped plate conditions, the ramped parameter Ra has a propensity to hike the fluid concentration.
- The skin friction drag τ upsurges with the increment of non-dimensional parameters Pr ; Sc , Gm , k , K , H , t , Q_i^* , Du , while an inverse impact was observed when increasing the value of the non-dimensional parameters β , Gr , M .
- It is spotted that the ascending values of time t , heat generation parameter H , radiation absorption Q_i^* and Dufour effect Du dominates the rate of heat transfer. On the other hand, Prandtl number Pr increases the rate of heat transfer.
- The Sherwood number observed to be enhanced under the impact of chemical reaction parameter k , Schmidt number Sc and time t .

Nomenclature

J	current density vector	t_o	critical time for rampdness
B_o	applied magnetic field strength	Du	Dufour number
\bar{B}	magnetic flux density	K'	permeability of porous medium
k	chemical reaction parameter	M	coefficient of viscosity
Pr	Prandtl number	D_M	mass diffusivity
H	heat generation parameter	C_s	concentration susceptibility
Q_i^*	radiation absorption parameter	U_o	characteristic plate velocity
β	Casson parameter	K_T	thermal diffusion ratio
K	non-dimensional permeability parameter	β'	co-efficient of thermal expansion
g	acceleration due to gravity	ν	kinematic viscosity

APPENDIX

$$G = G(\delta, I + a, y, t) = e^{at} \frac{1}{2} \left[e^{\sqrt{\delta(a+I)y}} \operatorname{erfc} \left(\frac{\sqrt{\delta y}}{2\sqrt{t}} + \sqrt{(a+I)t} \right) + e^{-\sqrt{\delta(a+I)y}} \operatorname{erfc} \left(\frac{\sqrt{\delta y}}{2\sqrt{t}} - \sqrt{(a+I)t} \right) \right]$$

$$\psi(\lambda_2, \beta, y, t) = \frac{1}{2} \left[e^{\sqrt{\lambda_2 \beta y}} \operatorname{erfc} \left(\frac{\sqrt{\lambda_2 y}}{2\sqrt{t}} + \sqrt{\beta t} \right) + e^{-\sqrt{\lambda_2 \beta y}} \operatorname{erfc} \left(\frac{\sqrt{\lambda_2 y}}{2\sqrt{t}} - \sqrt{\beta t} \right) \right]$$

$$\psi(\lambda_2, \beta, y, t-1) = \frac{1}{2} \left[e^{\sqrt{\lambda_2 \beta y}} \operatorname{erfc} \left(\frac{\sqrt{\lambda_2 y}}{2\sqrt{(t-1)}} + \sqrt{\beta(t-1)} \right) + e^{-\sqrt{\lambda_2 \beta y}} \operatorname{erfc} \left(\frac{\sqrt{\lambda_2 y}}{2\sqrt{(t-1)}} - \sqrt{\beta(t-1)} \right) \right] H$$

$$f(\lambda_1, k, y, t) = \left(\frac{t}{2} + \frac{y}{4} \sqrt{\frac{\lambda_1}{k}} \right) e^{\sqrt{\lambda_1 k y}} \operatorname{erfc} \left(\frac{y}{2} \sqrt{\frac{\lambda_1}{t}} + \sqrt{kt} \right) + \left(\frac{t}{2} - \frac{y}{4} \sqrt{\frac{\lambda_1}{k}} \right) e^{-\sqrt{\lambda_1 k y}} \operatorname{erfc} \left(\frac{y}{2} \sqrt{\frac{\lambda_1}{t}} - \sqrt{kt} \right)$$

$$f(\lambda_1, k, y, t-1) = \left[\left(\frac{(t-1)}{2} + \frac{y}{4} \sqrt{\frac{\lambda_1}{k}} \right) e^{\sqrt{\lambda_1 k y}} \operatorname{erfc} \left(\frac{y}{2} \sqrt{\frac{\lambda_1}{(t-1)}} + \sqrt{k(t-1)} \right) + \left(\frac{(t-1)}{2} - \frac{y}{4} \sqrt{\frac{\lambda_1}{k}} \right) e^{-\sqrt{\lambda_1 k y}} \operatorname{erfc} \left(\frac{y}{2} \sqrt{\frac{\lambda_1}{(t-1)}} - \sqrt{k(t-1)} \right) \right] H$$

$$V(\delta, I, a, t) = -e^{at} \left[\sqrt{\frac{\delta}{\pi t}} e^{-\delta(I+a)t} + \sqrt{\delta(I+a)} \operatorname{erf}(\sqrt{(I+a)t}) \right]$$

$$H = \operatorname{Heaviside}(t-1) = \begin{cases} 1, & t > 1 \\ \frac{1}{2}, & t = 0 \\ 0, & t < 1 \end{cases}$$

$$Y(\lambda_2, \beta, t) = - \left[\sqrt{\frac{\lambda_2}{\pi t}} e^{-\beta t} + \sqrt{\lambda_2 \beta} \operatorname{erf}(\sqrt{\beta t}) \right]$$

$$Y(\lambda_2, \beta, t-1) = - \left[\sqrt{\frac{\lambda_2}{\pi(t-1)}} e^{-\beta(t-1)} + \sqrt{\lambda_2 \beta} \operatorname{erf}(\sqrt{\beta(t-1)}) \right] H$$

$$\xi(\lambda_1, k, t) = - \left[\sqrt{\frac{\lambda_1}{4k}} \operatorname{erf}(\sqrt{kt}) + t \sqrt{\lambda_1 k} \operatorname{erf}(\sqrt{kt}) + \sqrt{\frac{t \lambda_1}{\pi}} e^{-kt} \right]$$

$$\xi(\lambda_1, k, t-1) = - \left[\sqrt{\frac{\lambda_1}{4k}} \operatorname{erf}(\sqrt{k(t-1)}) + (t-1) \sqrt{\lambda_1 k} \operatorname{erf}(\sqrt{k(t-1)}) + \sqrt{\frac{(t-1) \lambda_1}{\pi}} e^{-k(t-1)} \right] H$$

ORCID

©Dibya Jyoti Saikia, <https://orcid.org/0000-0001-6067-5390>; ©Nazibuddin Ahmed, <https://orcid.org/0000-0002-0924-4402>

REFERENCES

- [1] H. Alfven, "Existence of electromagnetic-hydrodynamic waves," *Nature*, **150**, 405-406 (1942). <https://doi.org/10.1038/150405d0>
- [2] G.S. Seth, Md.S. Ansari, and R. Nandkeolyar, "MHD natural convection flow with radiative heat transfer past an impulsively moving plate with ramped wall temperature," *Heat and mass transfer*, **47**, 551-561 (2011). <https://doi.org/10.1007/s00231-010-0740-1>
- [3] B.S. Goud, "Thermal radiation influences on MHD stagnation point stream over a stretching sheet with slip boundary conditions," *International Journal of Thermofluid Science and Technology*, **7**(2), 070201 (2020). <https://doi.org/10.36963/IJTST.2020070201>
- [4] C. Rath, A. Nayak, and S. Panda, "Impact of viscous dissipation and Dufour on MHD natural convective flow past an accelerated vertical plate with Hall current," *Heat Transfer*, **51**(6), 5971-5995 (2022). <https://doi.org/10.1002/htj.22577>
- [5] J.K. Singh, G.S. Seth, and P. Rohidas, "Impacts of time varying wall temperature and concentration on MHD free convective flow of a rotating fluid due to moving free-stream with hall and ion-slip currents," *International Journal of Thermofluid Science and Technology*, **6**(3), 19060301 (2019). <https://doi.org/10.36963/IJTST.19060301>
- [6] M.V. Krishna, N.A. Ahamad, and A.J. Chamkha, "Radiation absorption on MHD convective flow of nanofluids through vertically travelling absorbent plate," *Ain Shams Engineering Journal*, **12**, 3043-3056 (2021). <https://doi.org/10.1016/j.asej.2020.10.028>
- [7] S.R. Rao, G. Vidyasagar, and G.V.S.R. Deekshitulu, "Unsteady MHD free convection Casson fluid flow past an exponentially accelerated infinite vertical porous plate through porous medium in the presence of radiation absorption with heat generation/absorption," *Materials Today: Proceedings*, **42**, 1608-1616 (2021). <https://doi.org/10.1016/j.matpr.2020.07.554>
- [8] M.F. Endalew, and A. Nayak, "Thermal radiation and inclined magnetic field effects on MHD flow past a linearly accelerated inclined plate in a porous medium with variable temperature," *Heat Transfer - Asian Research*, **48**(1), 42-61 (2019). <https://doi.org/10.1002/htj.21367>
- [9] H.R. Kataria, and H.R. Patel, "Effects of chemical reaction and heat generation/absorption on magnetohydrodynamic (MHD) Casson fluid flow over an exponentially accelerated vertical plate embedded in porous medium with ramped wall temperature and ramped surface concentration," *Propulsion and power research*, **8**, 35-46 (2019). <https://doi.org/10.1016/j.jprr.2018.12.001>

- [10] J.-C. Zhou, A. Abidi, Q.-H. Shi, M.R. Khan, A. Rehman, A. Issakhov, and A.M. Galal, "Unsteady radiative slip flow of MHD Casson fluid over a permeable stretched surface subject to a non-uniform heat source," *Case Studies in Thermal Engineering*, **26**, 101141 (2021). <https://doi.org/10.1016/j.csite.2021.101141>
- [11] C. Sulochana, S.R. Aparna, and N. Sandeep, "Heat and mass transfer of magnetohydrodynamic Casson fluid flow over a wedge with thermal radiation and chemical reaction," *Heat transfer*, **50**, 3704-3721 (2021). <https://doi.org/10.1002/htj.22049>
- [12] R. Reyaz, Y.J. Lim, A.Q. Mohamad, M. Saqib, and S. Shafie, "Caputo fractional MHD Casson fluid flow over an oscillating plate with thermal radiation," *Journal of Advanced Research in Fluid Mechanics and Thermal Sciences*, **85**, 145-158 (2021). https://semarakilmu.com.my/journals/index.php/fluid_mechanics_thermal_sciences/article/view/8087
- [13] J. Bodduna, and C.S. Balla, "Bioconvection in a porous square cavity containing gyrotactic microorganisms under the effects of heat generation/absorption," *Proceedings of the Institution of Mechanical Engineers, Part E: Journal of Process Mechanical Engineering*, **235**, 1534-1544 (2021). <https://doi.org/10.1177/09544089211007326>
- [14] k. Ali, S. Ahmad, K.S. Nisar, A.A. Faridi, and M. Ashraf, "Simulation analysis of MHD hybrid $\text{CuAl}_2\text{O}_3/\text{H}_2\text{O}$ nanofluid flow with heat generation through a porous media," *International Journal of Energy Research*, **45**, 19165-19179 (2021). <https://doi.org/10.1002/er.7016>
- [15] M.R. Khan, S. Mao, W. Deebani, and A.M.A. Elsiddieg, "Numerical analysis of heat transfer and friction drag relating to the effect of Joule heating, viscous dissipation and heat generation/absorption in aligned MHD slip flow of a nanofluid," *International Communications in Heat and Mass Transfer*, **131**, 105843 (2022). <https://doi.org/10.1016/j.icheatmasstransfer.2021.105843>
- [16] M.K. Nayak, A.A. Hakeem, and B. Ganga, "Influence of non-uniform heat source/sink and variable viscosity on mixed convection flow of third grade nanofluid over an inclined stretched Riga plate," *International Journal of Thermofluid Science and Technology*, **6**(4), 19060401 (2019). <https://doi.org/10.36963/IJTST.19060401>
- [17] A. Nayak, S. Panda, and D.K. Phukan, "Soret and Dufour effects on mixed convection unsteady MHD boundary layer flow over stretching sheet in porous medium with chemically reactive species," *Applied Mathematics and Mechanics*, **35**(7), 849-862 (2014). <https://doi.org/10.1007/s10483-014-1830-9>
- [18] N.A. Ahammad, and M.V. Krishna "Numerical investigation of chemical reaction, Soret and Dufour impacts on MHD free convective gyrating flow through a vertical porous channel," *Case Studies in Thermal Engineering*, **28**, 101571 (2021). <https://doi.org/10.1016/j.csite.2021.101571>
- [19] M. Jawad, A. Saeed, P. Kumam, Z. Shah, and A. Khan, "Analysis of boundary layer MHD Darcy-Forchheimer radiative nanofluid flow with Soret and DuFour effects by means of Marangoni convection," *Case Studies in Thermal Engineering*, **23**, 100792 (2021). <https://doi.org/10.1016/j.csite.2020.100792>
- [20] N. Ahmed, and D.J. Saikia, "Unsteady MHD free convective flow past a moving vertical plate in a porous medium with radiation and chemical reaction including arbitrary thermal and solutal ramped condition," *Heat Transfer*, **51**, 6893-6914 (2022). <https://doi.org/10.1002/htj.22629>
- [21] C. Rath, and A. Nayak, "Transient natural convective flow of a radiative viscous incompressible fluid past an exponentially accelerated porous plate with chemical reaction species," *Heat Transfer*, **52**(1), 467-494 (2023). <https://doi.org/10.1002/htj.22703>
- [22] D. Gopal, S. Saleem, S. Jagadha, F. Ahmad, A.O. Almatroud, and N. Kishan, "Numerical analysis of higher order chemical reaction on electrically MHD nanofluid under influence of viscous dissipation," *Alexandria Engineering Journal*, **60**, 1861-1871 (2021). <https://doi.org/10.1016/j.aej.2020.11.034>
- [23] N.G. Reddy, V.S. Rao, and B.R. Reddy, "Chemical reaction impact on MHD natural convection flow through porous medium past an exponentially stretching sheet in presence of heat source/sink and viscous dissipation," *Case studies in thermal engineering*, **25**, 100879 (2021). <https://doi.org/10.1016/j.csite.2021.100879>
- [24] Sehra, S. Ul Haq, S.I.A. Shah, K.S. Nisar, S.U. Jan, and I. Khan, "Convection heat mass transfer and MHD flow over a vertical plate with chemical reaction, arbitrary shear stress and exponential heating," *Scientific Reports*, **11**, 1-11 (2021). <https://doi.org/10.1038/s41598-021-81615-8>
- [25] P.S. Reddy, and A.J. Chamkha, "Soret and Dufour effects on MHD convective flow of Al_2O_3 -water and TiO_2 -water nanofluids past a stretching sheet in porous media with heat generation/absorption," *Advanced Powder Technology*, **27**(4), 1207-1218 (2016). <http://dx.doi.org/10.1016%2Fj.apt.2016.04.005>
- [26] O. Mopuri, R.K. Madhu, M.R. Peram, C. Ganteda, G. Lorenzini, and N.A. Sidik, "Unsteady MHD on convective flow of a Newtonian fluid past an inclined plate in presence of chemical reaction with radiation absorption and Dufour effects," *CFD Letters*, **14**(7), 62-76 (2022). <https://doi.org/10.37934/cfdl.14.7.6276>

ТОЧНИЙ АНАЛІЗ ПОТОКУ МГД КАСОНОВОЇ РІДИНИ ПОВЗ ЕКСПОНЕНЦІЙНО ПРИСКОРЕНУ ВЕРТИКАЛЬНУ ПЛАСТИНУ В ПОРИСТОМУ СЕРЕДОВИЩІ З ПОГЛИНАННЯМ, ТЕПЛОВИДІЛЕННЯМ ТА ДИФУЗІЙНО-ТЕРМОЕФЕКТАМИ З ТЕРМІЧНИМИ ТА РОЗЧИННИМИ РАМПОВИМИ УМОВАМИ

Діб'я Джйоті Саїкія^{а,b}, Назібуддін Ахмед^с, Архенду Кр. Нанді^б, Діп Джйоті Бора^а

^аДепартамент математики, Університет Гаухаті, Гувахаті 781014, Індія

^бДепартамент математики, коледж Басугаон, Басугаон-783372 Ассам, Індія

^сДепартамент математики, Університет Котона, Гувахаті 781001, Індія

Поточне дослідження спрямоване на вивчення впливу поглинання випромінювання, виділення тепла та числа Дюфура на МГД-потік рідини Кассона повз експоненційно прискорену вертикальну пластину в пористому середовищі з хімічною реакцією. Основні рівняння для імпульсу, енергії та концентрації розв'язуються за допомогою методу перетворення Лапласа. Вирази для тертя поверхні, швидкості теплообміну та швидкості масообміну також виділені та зображені у вигляді таблиці. Дослідження моделює, що параметр Кассона зменшує швидкість рідини, тоді як потік енергії через градієнт концентрації маси покращує проблему температурного поля потоку. Крім того, спостерігається розвиток температурного поля під впливом поглинання випромінювання та виділення тепла. Додатково графічно показано вплив різних безрозмірних параметрів на поле швидкості, температуру рідини та концентрацію частинок.

Ключові слова: МГД; поглинання випромінювання; Кассонова рідина; теплогенерація; ефект Дюфура